Resonant Thermal Transport Driven by Surface Phonon-Polaritons in a Cylindrical Cavity

Jose Ordonez-Miranda, Maelie Coral, Masahiro Nomura, Sebastian Volz

Resonant Thermal Transport Driven by Surface Phonon-Polaritons in a Cylindrical Cavity

Jose Ordonez-Miranda[1,2*], Maelie Coral[2], Masahiro Nomura[2,1] and Sebastian Volz[1,2]

[1]LIMMS, CNRS-IIS UMI 2820, The University of Tokyo, Tokyo, 153-8505, Japan.
[2]Institute of Industrial Science, The University of Tokyo, Tokyo, 153-8505, Japan.

*Corresponding author(s). E-mail(s): jose.ordonez@cnrs.fr;
Contributing authors: mcoral@iis.u-tokyo.ac.jp;
nomura@iis.u-tokyo.ac.jp; volz@iis.u-tokyo.ac.jp;

Abstract

The axial thermal conductance of a cylindrical cavity supporting the propagation of hybridized guided modes along its interface with SiO_2 is quantified and analyzed as a function of its radius and mean temperature. In contrast to the well-known radial thermal conductance, we show that the axial one increases with the cavity radius up to 1 cm, in which it takes its maximum that increases with temperature. A maximum thermal conductance of $\mathbf{289.4}$ $\mathrm{nWK^{-1}}$ is found at 500K, which is more than 3 orders of magnitude higher than the corresponding one found in the far-field regime. This top polariton thermal conductance along the cavity is comparable to the radiative one predicted by Planck's theory and thus represents a fundamental heat transport channel driven by hybridized guided modes able to amplify heat currents along a macroscale cylindrical cavity.

Keywords: Surface phonon-polaritons, Resonant thermal transport, Cylindrical Vacuum Gap, Polariton thermal conductance.

1 Introduction

Surface phonon-polaritons (SPhPs) are electromagnetic surface waves generated by the coupling of infrared photons with optical phonons at the interface of polar materials [1–3]. These surface excitations are able to propagate a distance much longer than the typical mean free paths of phonons and electrons, which makes of them powerful energy carriers [4–9]. In thermal radiation across a vacuum gap, for example, the evanescent coupling of SPhPs inside the gap can enhance the heat transport several orders of magnitude over the blackbody limit [10–15]. This remarkable enhancement appears in the near-field regime and has a wide variety of applications in thermophotovoltaics [16, 17], thermal computing [18] and photonics[19–21].

While the near-field radiation inside a gap is driven by the cross-plane propagation and coupling of SPhPs, their in-plane propagation can also be exploited to carry heat along surfaces, via propagative modes [4, 5, 22, 23]. Previous theoretical [4, 5] and experimental [24, 25] works showed that the SPhP contribution to the in-plane heat flux along polar nanofilms can actually compete with their phonon counterparts. This high SPhP contribution arises from the evanescent coupling between the SPhPs propagating along the two nanofilm surfaces, distances longer than the corresponding cross-plane ones outside of the nanofilm [5]. The SPhP coupling shows up not only in single nanofilms, but also in microscale structures, as is the case of a $10-\mu$m-thick silicon layer sandwiched by two SiO_2 nanofilms that was recently studied [26]. As a result of the strong coupling of SPhPs propagating along its two SiO_2 nanofilms, this $SiO_2/Si/SiO_2$ structure can efficiently enhances the in-plane SPhP heat transport to values ten times higher than the corresponding one of a single SiO_2 nanofilm. Taking into account that silicon is a non-absorbing material within a wide range of infrared frequencies relevant for the propagation of SPhPs [27], the coupling of these energy carriers via a vacuum gap is also expected to generate a significant heat current along its interfaces. Further, as the number of SPhP modes increases with the gap distance [1, 26, 28], their thermal activation and combined contribution to this heat current along a gap could even be comparable to the Planck's limit of thermal radiation, but it is not studied yet.

The goal of this work is to theoretically demonstrate the resonant behavior of the in-plane thermal conductance of a cylindrical vacuum gap, as a function of its radius a. In contrast to the well-known cross-plane thermal conductance, it is shown that the in-plane one exhibits its lowest values as $a \to 0$ and its highest one at about $a = 1$ cm. This thermal resonance occurs due to the thermal activation of hundreds of hybridized guided modes (HGMs), resulting from the interaction of SPhP modes with standing waves propagating outside and inside the cavity, respectively. Unlike the single mode supporting the SPhP heat transport along a nanofilm [22], these HGMs maximize their energy density and coupling for a macroscale cavity.

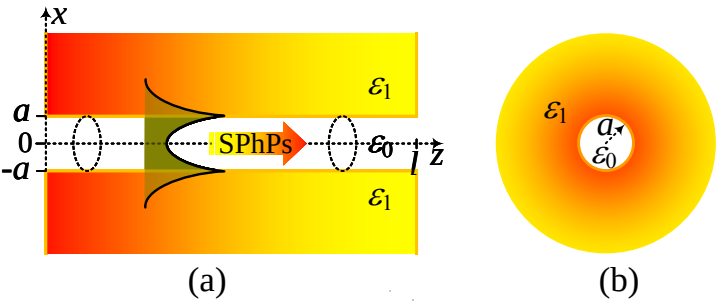

Fig. 1 (a) Scheme of a cylindrical cavity surrounded by a polar material of relative permittivity ε_1 and (b) its circular cross section. The cavity of radius a and relative permittivity ε_0 supports the propagation of SPhPs along the z axis.

2 Theoretical model

Let us consider a cylindrical cavity of radius a and relative permittivity ε_0 supporting the propagation of HGMs along its interface with a semi-infinite polar material of relative permittivity ε_1, as shown in Fig. 1. Assuming that the surface $z = 0$ of the polar material is uniformly heated up with a thermal source, the heat propagates along the z axis mainly and the in-plane thermal conductance G of the gap due to HGMs is given by [29]

$$G = \frac{1}{2\pi} \int \hbar\omega\tau(\omega) \frac{\partial f}{\partial T} d\omega, \tag{1}$$

where $\hbar$ is the Planck's constant divided by 2π, $f = [\exp(\hbar\omega/k_B T) - 1]^{-1}$ is the Bose-Einstein distribution function, T is the mean temperature, k_B is the Boltzmann constant, ω is the spectral frequency, and τ is the transmission probability given by

$$\tau = \frac{2}{\lambda}\left(1 - \frac{1 - \exp(-\lambda)}{\lambda}\right), \tag{2}$$

where $\lambda = l/\Lambda$ is the ratio between the cavity length l and the HGM in-plane propagation length $\Lambda = [2\mathrm{Im}(\beta)]^{-1}$. Equation (2) thus establishes that the transmission of HGMs along the cavity is fully determined by λ. In the diffusive regime ($\lambda = l/\Lambda \gg 1$), $\tau \approx 0$, while in the ballistic limit ($\lambda \ll 1$), $\tau \approx 1$. The HGM heat transport is hence enhanced along a system with a length l smaller than the HGM propagation length ($l \ll \Lambda$), as indicated by Eq. (1). In any case, according to Eqs. (1) and (2), the HGM thermal conductance depends on the material properties through $\tau(2l\mathrm{Im}(\beta))$, which is driven by the axial wave vector $\beta(\omega)$ given by the dispersion relation of HGMs propagating along the vacuum gap shown in Fig. 1. As G increases with this transmission probability, the optimal material configuration to maximize the HGM heat transport is given by a long propagation length (small $\mathrm{Im}(\beta)$). After solving the Maxwell equations under proper boundary conditions for the transverse magnetic polarization required for the existence of HGMs[4], the following

dispersion relation is obtained[28]

$$\frac{\varepsilon_0}{p_0}\frac{I_1(p_0a)}{I_0(p_0a)} + \frac{\varepsilon_1}{p_1}\frac{K_1(p_1a)}{K_0(p_1a)} = 0, \tag{3}$$

where I_n and K_n are the respective modified Bessel functions of first and second kind, p_m are the radial wave vectors given by $p_m^2 = \beta^2 - \varepsilon_m k_0^2$, with $k_0 = \omega/c$ and c being the wave vector and speed of light in vacuum, respectively. For a vacuum cavity ($\varepsilon_0 = 1$) surrounded by a lossless material ($\mathrm{Im}(\varepsilon_1) = 0$), as is the case of silicon ($\varepsilon_1 = 11.7$) [27], the solution of Eq. (3) does not correspond to confined waves and hence the cavity is unable to transport HGM energy. The existence ($\mathrm{Re}(p_m) > 0$) and propagation ($\Lambda > 0$) of HGMs can only be determined for lossy (absorbing) materials ($\mathrm{Im}(\varepsilon_1) > 0$), as is the case of a wide variety of polar dielectrics (i. e. SiO_2, SiC, SiN, hBN) [30]. In the "far-field" limit ($\mid p_m \mid a \gg 1$ or $a \to \infty$), the HGMs propagating along the cavity surface decouple and Eq. (3) reduce to the dispersion relation of HGMs propagating along a single interface (SI) $\varepsilon_0 p_1 + \varepsilon_1 p_0 = 0$ [28], which yields

$$\beta = k_0\sqrt{\frac{\varepsilon_0\varepsilon_1}{\varepsilon_0 + \varepsilon_1}}. \tag{4}$$

The HGM wave vector and hence the HGM thermal conductance G of an infinitely thick cavity become independent of the gap radius, as expected.

3 Results and discussion

The HGM propagation parameters and thermal conductance along a vacuum gap ($\varepsilon_0 = 1$) surrounded by SiO_2 are now numerically analyzed in comparison with their corresponding counterparts obtained for an infinitely thick gap ($a \to \infty$). Calculations are done for a cavity length $l = 1$ mm and with the experimental data of the complex and spectral SiO_2 permittivity reported in the literature [5, 30]. As the complex dispersion relation in Eq. (3) has multiple solutions (branches), we count them with "n", such that $n = 1$ represents the solution with the longest propagation length, $n = 2$ is the solution with the second longest propagation length, etc.

The dispersion relation $\beta_R = \mathrm{Re}(\beta)$ and in-plane propagation length Λ of HGMs propagating along a vacuum cavity are respectively shown in Figs. 2(a) and 2(b), for 5 representative branches (solutions) of the first 200 ones predicted by Eq. (3). Note that β_R increases with frequency, such that its first branch ($n = 1$) is pretty much superposed with the light line $k_0 = \omega/c$. Higher-order branches also exhibit this photon-like nature at high enough frequency but reduce the value and span of the wave vector at low frequency. Furthermore, the existence of hundreds of branches with β_R values comparable to those of the SI, for a relevant range of frequencies (see Fig. 4), indicates that the cavity is a better polariton thermal conductor than a SI. This is confirmed by Fig. 2(b), which shows that the propagation length of HGMs propagating

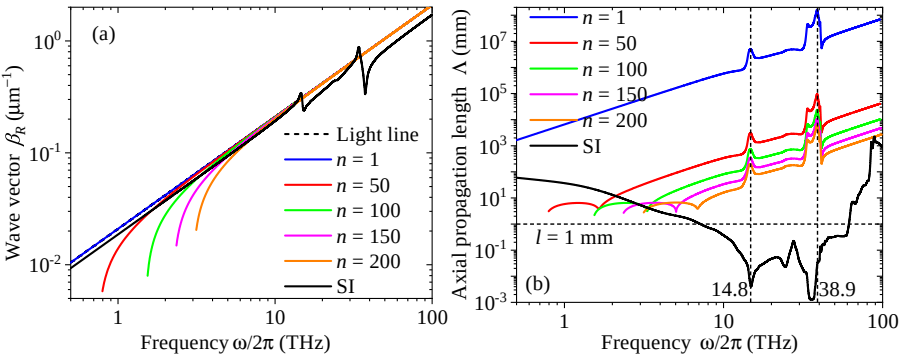

Fig. 2 Spectra of the axial (a) wave vector and (b) propagation length of HGMs propagating along a vacuum cavity surrounded by SiO_2, in comparison with the corresponding ones (black lines) obtained for a single interface ($a \to \infty$). Calculations were done for a cavity radius $a = 1$ cm and 5 representative branches of the first 200 ones predicted by Eq. (3).

along the cavity is generally greater than that along a SI (black line) and its maxima show up at frequencies (14.8 and 38.9 THz) where the SI propagation length exhibits its minima. These extreme values are induced by the dips of the real part of the SiO_2 permittivity [5, 30]. More importantly, as Λ is generally greater than the considered cavity length $l = 1$ mm, HGMs can travel along the whole cavity, which yields a transmission probability $\tau \approx 1$, as determined by Eq. (2). In contrast to the SI, the cavity thus allows to optimize and sum over several branches the two transmission probability τ enhancing the HGM heat transport along its surfaces.

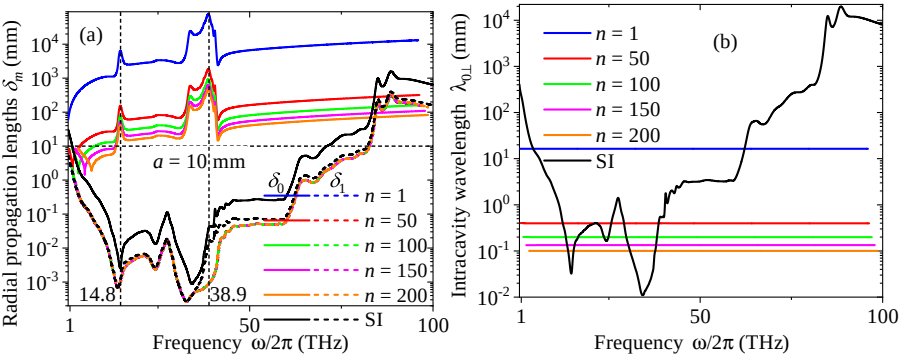

Fig. 3 Spectra of the radial (a) propagation lengths and (b) wavelength of HGMs propagating along a vacuum gap surrounded by SiO_2, in comparison with the corresponding ones (black lines) found for an infinitely thick cavity ($a \to \infty$). The solid and dashed lines in (a) represent the radial propagation lengths $\delta_m = [2\mathrm{Re}(p_m)]^{-1}$ inside ($m = 0$) and outside ($m = 1$) the cavity, respectively. Calculations were done for a cavity radius $a = 1$ cm and 5 representative branches of the first 200 ones predicted by Eq. (3).

Figure 3(a) shows the frequency dependence of the radial propagation length $\delta_m = [2\mathrm{Re}(p_m)]^{-1}$ inside ($m = 0$) and outside ($m = 1$) the cavity, for 5 representative branches of the first 200 ones. δ_m drives the exponential decay of the Poynting vector in the radial direction [28]. Note that δ_0 reduces as the branch order increases, while δ_1 remains invariant. As the SPhPs propagate a radial distance outside the cavity smaller than 1 cm ($\delta_1 < 1$ cm), for most relevant frequencies, the cylindrical wall can be considered infinitely thick, when the wall thickness is greater than 1 cm. This latter condition was assumed to derive the dispersion relation in Eq. (3) and is therefore required to validate the results reported in this work. On the other hand, Since δ_0 is generally greater than the considered cavity radius $a = 1$ cm, in particular for the first branch ($n = 1$), the HGMs propagating along the cavity interface are strongly coupled. This coupling indicates that the HGM thermal conductance in Eq. (1) represents the contribution of all HGM modes propagating not only along the interfaces, but also inside the cavity. According to Fig. 2(b), this coupling allows HGMs to propagate axial distances much longer than those in absence of it (SI case), with an intracavity radial wavelength $\lambda_{0\perp} = 2\pi\,[\mathrm{Im}(p_0)]^{-1}$ independent of frequency, as shown in Fig. 3(b). Note that shorter wavelengths are obtained for higher-order branches, such that $a = n\lambda_{0\perp}$, for $n = 2, 3, ...$ This condition maximizes the HGM Poynting vector along the cavity surface $r = a$ [28], and is analogous to the standing waves pattern of a guitar string. This maximization of the electromagnetic energy density of HGMs is directly correlated to the one of their thermal conductance determined by Eq. (1), since they exhibit relatively long axial propagation lengths (transmission $\tau \approx 1$) without a significant reduction of their axial wave vector (see Fig. 2). The standing modes shown in Fig. 3(b) are thus expected to optimize the HGM heat transport along the cavity. These cavity modes obtained for a cavity radius $a = 1$ cm are also present for other cavity radii, but not for all frequencies and branches, which indicates that the maximum HGM thermal conductance could be obtained for $a = 1$ cm, as confirmed below.

The contribution of 5 representative branches (solutions) of Eq. (3) to the spectrum G_ω of the HGM thermal conductance $G = \int G_\omega d\omega$ is shown in Fig. 4(a). Note that, for a cavity radius $a = 1$ cm, the multiple contributions to G_ω are higher than the corresponding one obtained for an infinitely thick cavity ($a \to \infty$) characterized by its peak at 27.7 THz for uncoupled HGMs. The 1-cm-radius cavity is therefore able to support the transport of more HGM thermal energy than this latter one, and actually more than a cavity of any other radius, as shown in Fig. 4(b). For the sake of accuracy, calculations for the 1-cm-radius cavity were done for the first 750 branches with a significant contribution ($G > 0.01$ nWK^{-1}). Other cavity radii involve a smaller number of branches and not all of them are cavity modes ($a = n\lambda_{0\perp}$) with a significant contribution, which hence yield a lower HGM thermal conductance. Note that the values of G for a cavity radius $a < 100$ µm are smaller than the ones for $a > 1$ m. This fact indicates that the high energy absorption of the SiO_2 cylindrical wall of a relatively small cavity has a stronger impact than the HGM

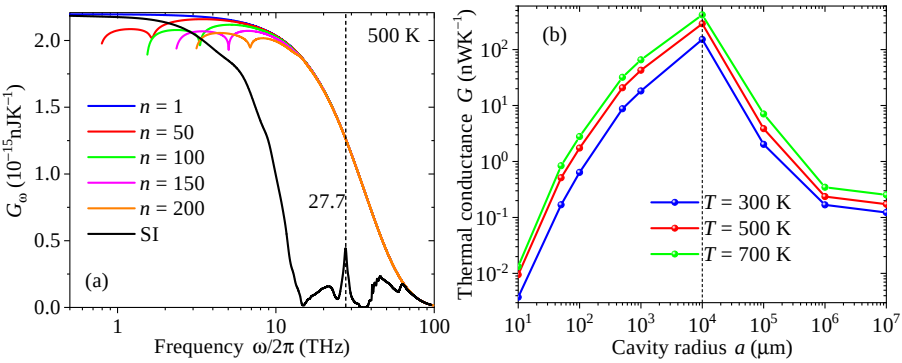

Fig. 4 (a) Spectrum of the HGM thermal conductance and (b) its integrated counterpart as a function of the radius of a cylindrical vacuum gap surrounded by SiO_2. The black line in (a) stands for the spectrum obtained for a thick gap ($a \to \infty$). Calculations in (a) were done for a cavity radius $a = 1$ cm and 5 representative branches of the first 200 ones predicted by Eq. (3). Calculations in (b) were done by summing up the contributions of the first 750 branches and for 3 representatives temperatures.

decoupling present for wide cavities, on the reduction of the HGM heat transport. More importantly, the total (sum over all modes) thermal conductance G reaches its maxima for a vacuum cavity of radius $a = 1$ cm, regardless of temperature. The peak of G appears at $a = 1$ cm for all temperatures, because the HGM propagation length reaches its longest values for this cavity radius. This maximization of the propagation distance leads to the of highest transmission and hence the highest values of G, as established by Eqs. (1) and (2). The maximum $G = 289.4$ nWK^{-1} is more than 3 orders of magnitude higher than the corresponding one ($G = 0.2$ nWK^{-1}) obtained for a thick cavity ($a \to \infty$) at 500 K. Higher or lower temperatures respectively yield higher or smaller HGM thermal conductances, as shown in Fig. 4(b). For the three considered temperatures, the maximum values of G are comparable to the corresponding ones that could be obtained by pure radiation [31]. This fact indicates that HGMs can be as good as thermal photons to transport heat along a cavity and therefore they could be used to amplify heat currents along macroscale gaps. The sizable gap radius ($a = 1$ cm) along with the relatively high maxima of the HGM thermal conductance are expected to facilitate its observation and application.

As the proposed cylindrical cavity supports the heat transport by hybridized guided modes and photons(regular thermal radiation), it could be applied to increase the evacuation and emission of heat currents, without significantly changing the temperature. This two-channel heat transport could therefore improve the thermal performance of conventional radiative exchangers, such as thermal fins and sinks commonly used in refrigerators, power engines, and electronic cooling. Finally, we point out that for a given surrounding material, the HGM heat transport along a cylindrical cavity is determined by its radius and length, while the one along a cavity between two parallel plates is driven by its thickness, length, and lateral width [31]. As a cavity

with uniform thickness could be difficult to implement in practice due to the possible misalignment of its plates, the cylindrical cavity provides a suitable geometry to guide and emit the SPhP thermal energy.

4 Conclusion

The resonant behavior of the in-plane thermal conductance of a cylindrical vacuum cavity supporting the propagation of hybridized guided modes has been studied as a function of the cavity radius. For a 1-cm-radius cavity and mean temperature of 500 K, a maximum thermal conductance of 289.4 nWK^{-1} has been found, which is more than 3 orders of magnitude higher than the corresponding one found in the far-field regime. This resonance is generated by the thermal excitation of hundreds of cavity modes that maximize the energy density and coupling of polaritons propagating along the cavity interface. Furthermore, it has been shown that hybridized guided modes are powerful energy carriers able to transport heat along the cavity as much as thermal photons and therefore they could be useful to enhance or evacuate heat currents along macroscale gaps.

Declarations

Ethical Approval

Not applicable.

Competing interests

The authors declare no competing interests.

Authors' contributions

J. O. M. and M. C. did the calculations, which were analyzed and interpreted by M. N. and S. V. Futher, J. O. M. wrote the manuscript.

Funding

This work is supported by the CREST Japan Science and Technology Agency, Grants No. JPMJCR19Q3 and No. JPMJCR19I1, and the French project ANR-19-CE09-0005 "EPolariton". This work is also supported by the JSPS core-to-core program (grant No. JPJSCCA20190006).

Availability of data and materials

The data that support the findings of this study are available from the corresponding author upon reasonable request.

References

[1] Agranovich, V.M.: Surface Polaritons. Elsevier, Amsterdam (2012)

[2] Ordonez-Miranda, J., Tranchant, L., Gluchko, S., Volz, S.: Energy transport of surface phonon polaritons propagating along a chain of spheroidal nanoparticles. Phys. Rev. B **92**, 115409–115413 (2015)

[3] Ordonez-Miranda, J., Tranchant, L., Joulain, K., Ezzahri, Y., Drevillon, J., Volz, S.: Thermal energy transport in a surface phonon-polariton crystal. Phys. Rev. B **93**, 035428 (2016)

[4] Chen, D.-Z.A., Narayanaswamy, A., Chen, G.: Surface phonon-polariton mediated thermal conductivity enhancement of amorphous thin films. Phys. Rev. B **72**, 155435 (2005)

[5] Ordonez-Miranda, J., Tranchant, L., Tokunaga, T., Kim, B., Palpant, B., Chalopin, Y., Antoni, T., Volz, S.: Anomalous thermal conductivity by surface phonon-polaritons of polar nano thin films due to their asymmetric surrounding media. J. Appl. Phys. **113**(8), 084311–084318 (2013)

[6] Yang, F., Sambles, J.R., Bradberry, G.W.: Long-range surface modes supported by thin films. Phys. Rev. B **44**, 5855–5872 (1991)

[7] Chen, D.Z.A., Chen, G.: Measurement of silicon dioxide surface phonon-polariton propagation length by attenuated total reflection. Appl. Phys. Lett. **91**, 121906–121909 (2007)

[8] Ordonez-Miranda, J., Tranchant, L., Antoni, T., Chalopin, Y., Volz, S.: Thermal conductivity of nano-layered systems due to surface phonon-polaritons. J. Appl. Phys. **115**, 054311–054315 (2014)

[9] Gluchko, S., Palpant, B., Volz, S., Braive, R., Antoni, T.: Thermal excitation of broadband and long-range surface waves on sio2 submicron films. Appl. Phys. Lett. **110**(26), 263108 (2017)

[10] Rousseau, E., Siria, A., Jourdan, G., Volz, S., Comin, F., Chevrier, J., Greffet, J.-J.: Radiative Heat Transfer at the Nanoscale

[11] Song, B., Thompson, D., Fiorino, A., Ganjeh, Y., Reddy, P., Meyhofer, E.: Radiative Heat Conductances Between Dielectric and Metallic Parallel Plates with Nanoscale Gaps

[12] Kittel, A., Müller-Hirsch, W., Parisi, J., Biehs, S.-A., Reddig, D., Holthaus, M.: Near-field heat transfer in a scanning thermal microscope. Phys. Rev. Lett. **95**, 224301 (2005)

[13] Fernández-Hurtado, V., García-Vidal, F.J., Fan, S., Cuevas, J.C.: Enhancing near-field radiative heat transfer with si-based metasurfaces. Phys. Rev. Lett. **118**, 203901 (2017)

[14] Ghashami, M., Geng, H., Kim, T., Iacopino, N., Cho, S.K., Park, K.: Precision measurement of phonon-polaritonic near-field energy transfer between macroscale planar structures under large thermal gradients. Phys. Rev. Lett. **120**, 175901 (2018)

[15] Ottens, R.S., Quetschke, V., Wise, S., Alemi, A.A., Lundock, R., Mueller, G., Reitze, D.H., Tanner, D.B., Whiting, B.F.: Near-field radiative heat transfer between macroscopic planar surfaces. Phys. Rev. Lett. **107**, 014301 (2011)

[16] Fiorino, A., Xu, L., Thompson, D., Mittapally, R., Reddy, P., Meyhofer, E.: Nanogap Near-field Thermophotovoltaics

[17] Lucchesi, C., Cakiroglu, D., Perez, J.-P., Taliercio, T., Tournie, E., Chapuis, P.-O., Vaillon, R.: Near-Field Thermophotovoltaic Conversion with High Electrical Power Density and Cell Efficiency Above 14%

[18] Ben-Abdallah, P., Biehs, S.-A.: Near-field thermal transistor. Phys. Rev. Lett. **112**, 044301 (2014)

[19] Rodriguez, A.W., Reid, M.T.H., Varela, J., Joannopoulos, J.D., Capasso, F., Johnson, S.G.: Anomalous near-field heat transfer between a cylinder and a perforated surface. Phys. Rev. Lett. **110**, 014301 (2013)

[20] Biehs, S.-A., Rousseau, E., Greffet, J.-J.: Mesoscopic description of radiative heat transfer at the nanoscale. Phys. Rev. Lett. **105**, 234301 (2010)

[21] Lim, M., Song, J., Lee, S.S., Lee, B.J.: Tailoring near-field thermal radiation between metallo-dielectric multilayers using coupled surface plasmon polaritons. Nat Commun. **9**, 4302 (2018)

[22] Guo, Y., Tachikawa, S., Volz, S., Nomura, M., Ordonez-Miranda, J.: Quantum of thermal conductance of nanofilms due to surface-phonon polaritons. Phys. Rev. B **104**, 201407 (2021)

[23] Ordonez-Miranda, J., Tranchant, L., Kim, B., Chalopin, Y., Antoni, T., Volz, S.: Quantized thermal conductance of nanowires at room temperature due to zenneck surface-phonon polaritons. Phys. Rev. Lett. **112**, 055901–055905 (2014)

[24] Tranchant, L., Hamamura, S., Ordonez-Miranda, J., Yabuki, T., Vega-Flick, A., Cervantes-Alvarez, F., Alvarado-Gil, J.J., Volz, S., Miyazaki,

K.: Two-dimensional phonon polariton heat transport. Nano Lett. **19**, 6924–6930 (2019)

[25] Wu, Y., Ordonez-Miranda, J., Gluchko, S., Anufriev, R., Meneses, D.D.S., Campo, L.D., Volz, S., Nomura, M.: Enhanced thermal conduction by surface phonon-polaritons. Sci. Adv. **6**, 4461 (2020)

[26] Tachikawa, S., Ordonez-Miranda, J., Wu, Y., Jalabert, L., Anufriev, R., Volz, S., Nomura, M.: High surface phonon-polariton in-plane thermal conductance along coupled films. Nanomaterials **10**, 1383 (2020)

[27] Dunlap, W.C., Watters, R.L.: Direct measurement of the dielectric constants of silicon and germanium. Phys. Rev. **92**, 1396 (1953)

[28] Yeh, C., I., S.F.: The Essence of Dielectric Waveguides. Springer, New York (2008)

[29] Guo, Y., Nomura, M., Volz, S., Ordonez-Miranda, J.: Heat transport driven by the coupling of polaritons and phonons in a polar nanowire. Energies **14**(16) (2021)

[30] Palik, E.D.: Handbook of Optical Constants of Solids. Academic Press, Orlando, Florida (1985)

[31] Volz, S., Nomura, M., Ordonez-Miranda, J.: Resonant polariton thermal transport along a vacuum gap. Phys. Rev. Appl. **18**, 051003 (2022)